Structural characteristics of ^{142}Ce through inelastic neutron scattering

J. R. Vanhoy, J. M. Anthony, B. M. Haas, B. H. Benedict, and B. T. Meehan
Department of Physics, United States Naval Academy, Annapolis, Maryland 21402

Sally F. Hicks, C. M. Davoren, and C. L. Lundstedt
Department of Physics, University of Dallas, Irving, Texas 75062
(Received 7 July 1995)

The excited levels of ^{142}Ce have been studied using the $(n,n'\gamma)$ reaction. Excitation functions, angular distributions, and Doppler shifts were measured for γ rays from levels up to an excitation energy of 3.3 MeV; multipole-mixing and branching ratios and transition rates were deduced. Theoretical predictions of electromagnetic transition rates were compared for the interacting boson model, the quasiparticle phonon model, and the particle-core coupling model with experimental values. Evidence is found supporting the fragmentation of mixed-symmetry strength among neighboring ^{142}Ce excited levels. This fragmentation is evinced in the 2^+ excitations through strong $M1$ transitions; however, the 3^+ mixed-symmetry strength is not manifested directly through strong $M1$ transitions, but rather is implied through model calculations. Candidates for multiphonon excitations are identified for the three-quadrupole and quadrupole-octupole phonon quintets.

PACS number(s): 25.40.Dn, 25.40.Fq, 27.80.+w, 28.20.Cz

I. INTRODUCTION

The $N=84$ isotones have been the subject of many theoretical [1–6] and experimental investigations [7,8] into the collective and particle nature of low-lying excitations in nuclei near the closed $N=82$ neutron shell. These nuclei became of considerable interest when Hamilton *et al.* [1] suggested that the 2_3^+ level in ^{140}Ba, ^{142}Ce, and ^{144}Nd exhibited isovector or mixed-symmetry (MS) properties consistent with predictions [9] of the interacting boson model-2 (IBM-2) within the U(5) vibrational limit. Further evidence supporting the 2_3^+ as a low-lying quadrupole MS state in ^{142}Ce came from Coulomb excitation studies by Vermeer *et al.* [8].

Experimental information on the $N=84$ isotones is sparse and restricted to level spins and parities and a few transition rates. Information regarding low-lying excitations in ^{142}Ce comes from Coulomb excitation [8,10], β decay [11,12], reactor-based $(n,n'\gamma)$ [13], and electron scattering [7]. Decay rates for other than ground-state transitions are quite limited for ^{142}Ce, especially for excitations above 2 MeV.

In this investigation of ^{142}Ce, experimental information is extended to approximately 3.3 MeV excitation. Electromagnetic transition rates for states having lifetimes in the range of a few femtoseconds to about one picosecond have been determined. This new information enables us to compare ^{142}Ce properties with various model predictions, to look for multiphonon excitations, and to investigate MS properties of the excited levels of this nucleus; new experimental information permits the examination of MS characteristics of low-lying 1^+ and 3^+ levels in this nucleus, as well as the possible fragmentation of MS quadrupole strength.

In Sec. II we briefly describe the experimental procedures used to extract level information. In Sec. III we present level discussions for those states in which there is debate about the experimental information. We then make comments regarding systematics in this nucleus. In Sec. IV we make detailed comparisons of the experimental information to model predictions. Results are summarized in Sec. V.

II. EXPERIMENTAL METHOD AND DATA REDUCTION

Measurements were made using the neutron scattering facility at the University of Kentucky 7 MV Van de Graaff Accelerator Laboratory. The ^{3}H$(p,n)^3$He reaction was used as a neutron source. The 42.3 g powdered $^{142}CeO_2$ sample was isotopically enriched to 93% and was packed into a thin-walled polyethylene container with a diameter of 2.4 cm and a height of 3.3 cm. Gamma rays were detected with a BGO Compton-suppressed n-type HpGe detector of 52% relative efficiency and an energy resolution of 2.1 keV FWHM at 1.33 MeV. The gain stability of the system was monitored at each angle using radioactive ^{56}Co and ^{152}Eu sources. Background lines were identified by scattering from a natural car-

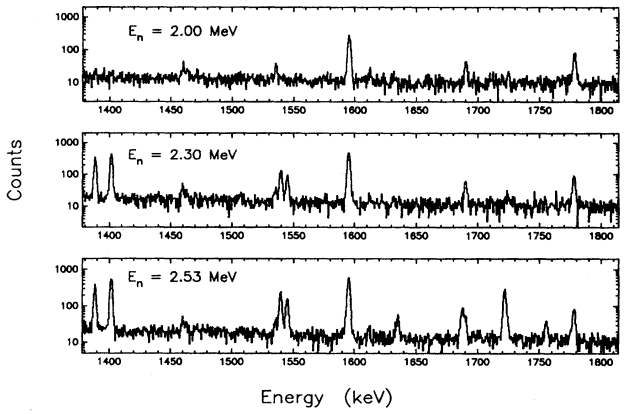

FIG. 1. A portion of γ-ray excitation function spectra from the ^{142}Ce$(n,n'\gamma)$ reaction for incident neutron energies of 2.00, 2.30, and 2.53 MeV. A detailed sequence of excitation function data guides the placement of levels and the assignment of transitions.

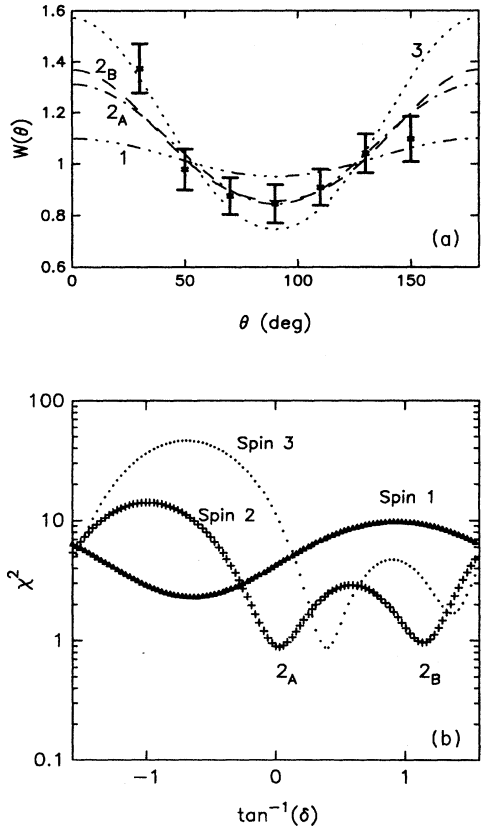

FIG. 2. (a) The top panel is a plot of the angular distribution of the 2164.8-keV transition. Best-fit curves for initial state spins of 1–3 are shown along with the experimental data. (b) The $E2/M1$ multipole-mixing ratio of the 2164.8-keV transition is deduced from this χ^2 vs $\tan^{-1}(\delta)$ plot. There are two solutions for decays from a spin-2 initial state which are denoted by 2_A and 2_B.

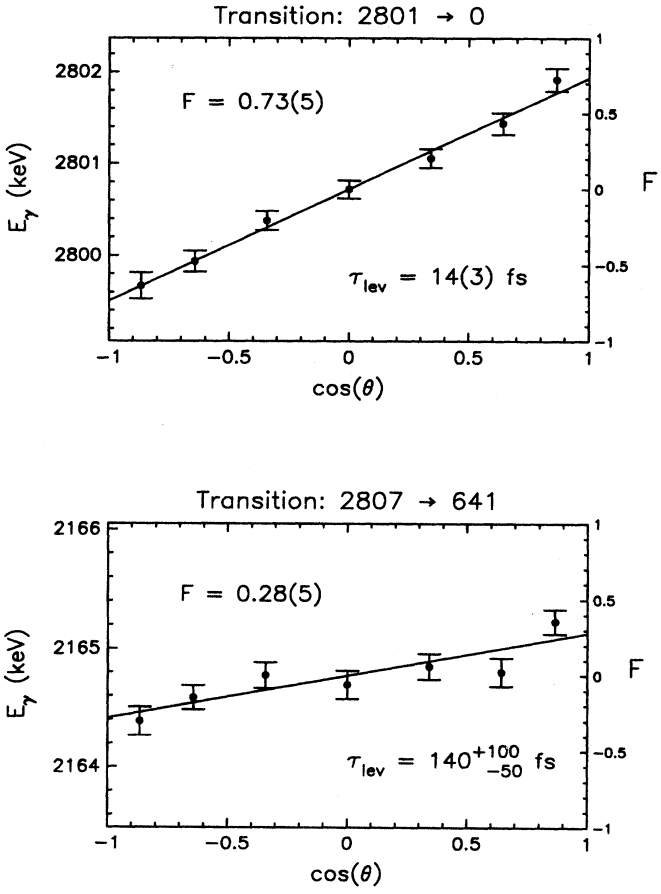

FIG. 3. Doppler-shift data for the 2801.0-keV to ground-state transition and for the 2806.6-keV to 641.3-keV transition. The experimental value of the Doppler-shift attentuation factor $F(\tau)$ is determined from the slope of the best-fit line. The Winterbon formalism is used to relate $F(\tau)$ to the meanlife τ.

bon sample. The neutron scattering facilities, time-of-flight background suppression, neutron monitoring, and data reduction techniques have been described elsewhere [14].

Excitation functions measured for incident neutron energies between 2.0 – 2.5 MeV in 75 keV steps and between 2.7 – 3.3 MeV in 50 keV steps were used to place γ rays in the decay scheme and to determine level energies. Figure 1 shows an example of excitation function data for neutron energies of 2.00, 2.30, and 2.53 MeV.

Angular distributions of deexcitation γ rays were measured at neutron energies of 2.85, 3.05, and 3.30 MeV. The angular distributions were fit to even-order Legendre polynomial expansions and compared to theoretical calculations from the statistical model code CINDY [15] in order to deduce level spins and parities and to extract multipole-mixing ratios. Optical model parameters used in the calculations were taken from Ref. [16]. The measured angular distribution of the 2164.8-keV transition along with theoretical curves for different spin possibilities of the initial level are shown in Fig. 2(a). Figure 2(b) is an example of the χ^2 vs $\tan^{-1}(\delta)$ plot used to determine the multipole-mixing ratio for this same transition.

Level lifetimes were extracted using the Doppler-shift attenuation method following inelastic neutron scattering. At the recoil velocities present in this experiment, the γ-ray peaks have centroids with the following angular dependence:

$$E_\gamma(\theta)=E_o[1+F(\tau)\beta\cos(\theta)],$$

where E_o is the unshifted γ-ray energy, $F(\tau)$ is the Doppler-shift attenuation factor, $\beta=v_{\text{c.m.}}/c$, θ is the γ-ray emission angle with respect to the incident neutron beam, and $E_\gamma(\theta)$ is the γ-ray energy measured at angle θ. Lifetimes were determined by comparing experimental and theoretical Doppler-shift attenuation factors. Theoretical values of $F(\tau)$ were calculated using the theory of Winterbon [17], since this method has been shown to yield reliable lifetimes with oxide targets [18]. Doppler-shift data for the 2800.4-keV ground-state transition and for the 2164.8-keV transition between the 2806.6-keV and 641.3-keV levels are shown in Fig. 3.

Experimental information, including γ-ray intensities, a_2 and a_4 angular distribution coefficients, experimental Doppler-shift attenuation factors, and transition energies, derived from the excitation functions and angular distributions for all observed levels is available from the authors and will

be submitted to the National Nuclear Data Compilation Center (NNDC). Electromagnetic transition rates, branching and mixing ratios, and lifetimes determined from these data are listed in Table I.

III. LEVEL DISCUSSION

Experimental information for all observed levels is given in the tables; only those states which merit special attention are discussed in detail below.

New levels were observed at 2330.5, 2374.9, 2576.4, 2774.0, 2784.9, 2860.0, 2869.1, 2934.0, 2956.5, 3009.9, 3042.4, 3052.0, 3109.8, 3125.7, 3144.9, and 3155.7 keV. The transitions associated with these new states are listed in Table I. Several additional levels are listed in Table I above 3150-keV excitation that are observed near production threshold. Low yields make transition placements and good energy determinations difficult for them.

Previously assigned levels not observed in this experiment are the 2014-, 2807-, and 2907-keV states. The 2014-keV state was also not observed by Alhamidi *et al.* [13]. The 2807- and 2907-keV levels were reported by Alhamidi *et al.* [13]; we see transitions associated [13] with the decays of these states at lower thresholds.

1536.9-keV 2_2^+ state. Decays of the 1536.9 keV level to both the ground and first-excited states were observed in this experiment. The measured lifetime of $\tau = 240^{+1600}_{-130}$ fs has a large uncertainty because of the curvature in the $F(\tau)$ curve near 1 ps. The NNDC compilation [19] value of $\tau < 1.2$ ps was used along with our experimental branching and mixing ratios to determine lower limits of $B(E2)$ and $B(M1)$ values. A previous measurement had set an upper limit of $B(E2;2_2^+ \rightarrow 0_1^+) < 0.36$ W.u. [8] for the ground-state decay rate.

1652.9-keV 3^- state. The ground state branch from this state has not yet been observed in γ-decay experiments. We set the branching ratio as $<0.1\%$.

2004.9-keV 2_3^+ state. Previously measured values of $B(E2;2_3^+ \rightarrow 0_1^+) = 3.18(50)$ W.u. [8] and $B(E2;2_3^+ \rightarrow 2_1^+) = 2.82(11)$ W.u. [20–22] were determined by Coulomb excitation and electron scattering, respectively. Our measurements resulted in a somewhat smaller value of $B(E2;2_3^+ \rightarrow 0_1^+) = 2.5(2)$ W.u. Additionally, our measured value of $B(E2;2_3^+ \rightarrow 2_1^+) = 2.6(3)$ W.u. is significantly smaller than $B(E2;2_3^+ \rightarrow 2_1^+) = 7.5 \pm 2.5$ W.u. reported by Vermeer *et al.* [8].

Previous investigations of $B(E2)$ strengths in the $N=84$ isotones have indicated that the ratio of $B(E2;2_3^+ \rightarrow 0_1^+)/B(E2;2_3^+ \rightarrow 2_1^+)$ is about 8 times higher for ^{142}Ce than for the other $N=84$ isotones (see for instance Fig. 3 in Ref. [5]). The ratio of 0.96 determined in this work, in contrast, is in excellent agreement with the trend for the other $N=84$ isotones. This same ratio as determined by Vermeer *et al.* [8] is 0.42 which is less than half the value for the other $N=84$ isotones.

2044.5-keV 4_2^+ state. The 4_2^+ level at 2044.5 keV decays into the 2_1^+ state and weakly into the 4_1^+ state. A possible decay into the 2_2^+ level is evident as a doublet on the side of the 511-keV e^+e^- annihilation line in the spectra, but it was not possible to extract reliable yields. We estimate that this resulting $B(E2)$ could easily be a few Weisskopf units.

2210-keV 6 state. This level was proposed by Alhamidi *et al.* [13] based on 467- and 991-keV transitions. Our data show markedly different excitation functions for these two γ rays, with the 991.7-keV transition turning on about two-hundred keV higher than the 467.6-keV γ ray. The 467.6-keV γ ray first appears at $E_n = 2.53$ MeV in our data and cannot be definitively placed; this leaves the 2210-keV state in question since a spin-6 state cannot definitely be eliminated or confirmed.

2398.7-keV 1^+ state. A 394.0-keV transition previously assigned [19] to this level was observed to have a much different excitation function than the other γ rays associated with this state. It has tentatively been reassigned to the 2576.4-keV level.

2540.2-keV 4^+ state. This state decays via 1898.6- and 1320.3-keV transitions. A 358.7-keV line has an excitation function similar to the other two transitions and may be associated with this level. This 358.7-keV transition was previously assigned to the 2569-keV level; this assignment depends on the existence of the 2210-keV level, a state for which we have no clear evidence.

2542.8-keV 1 state and 2543.3-keV 2^+ state. A close doublet of states has been suggested by Alhamidi *et al.* [13] on the basis of discrepancies between results of ^{142}La β-decay experiments [12] and by an apparently elevated population of a "2543-keV" level. Gamma rays of 2542, 1901, and 1323 keV had been placed with this doublet. In this experiment, the doublet was revealed via separate shifts of γ-ray energies during the Doppler-shift measurements.

Both levels have ground-state transitions. The 2542.8-keV state is very short lived and the resulting large Doppler shift separates the doublet at back angles. The angular distribution of the 2542.8-keV ground-state decay fixes the level spin to be 1.

A 1902.1-keV transition is placed with the 2543.3-keV state based on energy differences. There is no evidence for a similar transition to the first excited state from the 2542.8-keV state with a Doppler shift consistent with that of the 2542.8-keV line and a yield greater than $\approx$ 10% of the 1902.1-keV transition.

A 1323.9-keV transition is placed with the 2543.3-keV state. There is no evidence of a similar transition from the 2542.8-keV state.

2570.2-keV state. The 358.7-keV transition previously associated with this level rests on the existence of the 2210-keV state, which we do not see.

2768.0-keV (1-3) state. Deexcitation is observed via 2126.5-, 1231.5-, and 1115.0-keV transitions. The 1115.0-keV transition is a new assignment. Branching ratios may not be reliable as the 1115.0-keV line contains a background component.

2842.6-keV 2,3 state. The branching ratios for this level may be unreliable due to background interference with the 838.0-keV line.

2934.0-keV (2-4) state. Two transitions are placed from this state: 2292.7 keV and 1398.8 keV. The 1398.8-keV transition appears as a small peak on the side of the 1403.0-keV line in the spectra. This results in a rather large energy uncertainty for the transition, and one cannot rule out its placement with the 3052.0-keV level described below.

3052.0-keV state. Transitions of 2410.4, 1832.6, and

TABLE I. Level and transition information for ^{142}Ce. Level uncertainties in the last digit are given in parentheses. Uncertainties in transition energies are <0.1 keV for well-resolved γ rays below 1500 keV. Uncertainties in excitation energies are typically <0.2 keV for levels with decays into the first excited state. Tentative assignments are indicated by parentheses.

J^π	E_x (keV)	E_γ (keV)	E_f (keV)	BR %	$\tan^{-1}(\delta)$ [a]	τ [b] (fs)	$B(M1)$ (W.u.)	$B(E2)$ (W.u.)
2^+	641.3(1)	641.3	0	100		8200^{+820}_{-820}		$2.1^{+0.2}_{-0.2}E+1$
4^+	1219.5(1)	578.1	641	100		10800^{+900}_{-900}		$2.7^{+0.3}_{-0.2}E+1$
2^+	1536.9(4)	1537.4	0	1		<1200		$>2.3E-2$
		895.1	641	99	$-0.97^{+0.25}_{-0.25}$		$>1.2E-2$	$>1.9E+1$
3^-	1652.9(2)	1011.7	641	87		>2600	$BE1<1.2E-4$	
		433.2	1219	13			$BE1<2.2E-4$	
6^+	1743.0(1)	523.5	1219	100				
2^+	2004.9(1)	2004.9	0	28		65^{+7}_{-6}		$2.5^{+0.2}_{-0.2}$
		1363.6	641	70	$-0.25^{+0.13}_{-0.15}$		$0.13^{+0.01}_{-0.01}$	$2.6^{+0.3}_{-0.3}$
		352.1	1653	2			$BE1=2.6^{+0.3}_{-0.3}E-3$	
0^+	2031.0(1)	1389.7	641	100		250^{+220}_{-90}		$1.5^{+0.8}_{-0.7}E+1$
4^+	2044.5(1)	1403.0	641	97		470^{+160}_{-100}		$7.2^{+2.0}_{-1.8}$
		825.2	1219	3	$-0.06^{+0.97}_{-0.22}$		$3.6^{+1.0}_{-0.9}E-3$	$1.1^{+0.3}_{-0.3}E-2$
4^+	2112.0(1)	892.5	1219	100	$-0.41^{+0.03}_{-0.07}$	530^{+440}_{-170}	$7.1^{+3.4}_{-3.2}E-2$	$10.0^{+4.7}_{-4.5}$
5^-	2124.9(2)	905.6	1219	80		>590	$BE1<6.6E-4$	
		(471)	1653	10				$<1.38E+2$
		381.8	1743	9			$BE1<9.8E-4$	
3^+	2182.1(5)	1540.9	641	39	$0.09^{+0.04}_{-0.03}$	380^{+800}_{-160}	$8.8^{+6.6}_{-6.0}E-3$	$1.8^{+1.3}_{-1.2}E-2$
		962.5	1219	46	$-0.44^{+0.13}_{-0.69}$		$3.5^{+2.6}_{-2.4}E-2$	$5.0^{+3.7}_{-3.4}$
		645.6	1537	12	$-0.38^{+0.07}_{-0.09}$		$3.2^{+2.4}_{-2.2}E-2$	$7.3^{+5.4}_{-4.9}$
		528.7	1653	4			$BE1=2.5^{+1.9}_{-1.7}E-4$	
1^-	2187.6(1)	2187.4	0	58		16^{+3}_{-3}	$BE1=1.2^{+0.3}_{-0.2}E-3$	
		1546.3	641	41			$BE1=2.4^{+0.5}_{-0.4}E-3$	
		(534)	1653	<0.3				$<7.9E+1$
4^+	2278.0(1)	1636.8	641	71		120^{+70}_{-40}		$9.7^{+4.4}_{-3.6}$
		1058.5	1219	29	$1.13^{+0.03}_{-0.06}$		$1.2^{+0.6}_{-0.4}E-2$	$2.9^{+1.3}_{-1.1}E+1$
3	2330.5(1)	1689.2	641	70	$-0.16^{+0.12}_{-0.12}$	300^{+310}_{-110}	$1.5^{+0.9}_{-0.8}E-2$	$8.2^{+4.7}_{-4.2}E-2$
		793.4	1537	30	$0.35^{+0.19}_{-0.16}$		$5.6^{+3.2}_{-2.9}E-2$	$7.1^{+4.1}_{-3.6}$
2^+	2364.9(1)	2364.8	0	24		23^{+4}_{-3}		$2.6^{+0.4}_{-0.3}$
		1723.6	641	76	$-0.03^{+0.09}_{-0.10}$		$0.20^{+0.03}_{-0.03}$	$3.7^{+0.6}_{-0.5}E-2$
6	2374.9(2)	1155.7	1219	52	$-0.09^{+0.06}_{-0.10}$	–		
		631.8	1743	47	$-1.38^{+0.41}_{-0.19}$			
4^-	2384.5(2)	1165.3	1219	16		87^{+110}_{-40}	$BE1=4.2^{+4.0}_{-2.6}E-4$	
		731.5	1653	79	$-0.69^{+0.19}_{-0.19}$		$0.44^{+0.38}_{-0.25}$	$3.3^{+2.9}_{-1.9}E+2$
		202.3	2182	5			$BE1=2.5^{+2.1}_{-1.4}E-2$	
1^+	2398.7(3)	2398.5	0	78		110^{+30}_{-20}	$1.7^{+0.4}_{-0.4}E-2$	
		1757.1	641	14	$-1.00^{+0.10}_{-0.10}$		$2.2^{+0.6}_{-0.5}E-3$	$1.0^{+0.3}_{-0.2}$
		862.1	1537	8	$0.03^{+0.05}_{-0.05}$		$3.6^{+1.0}_{-0.9}E-2$	$2.6^{+0.7}_{-0.6}E-2$
4^+	2540.2(5)	1898.6	641	14		59^{+26}_{-17}		$1.8^{+0.7}_{-0.6}$
		1320.3	1219	18				$1.4^{+0.6}_{-0.4}E+1$
		(358.7)	2182	67	-0.53			
1	2542.8(2)	2542.8	0	100		<20		
2^+	2543.3(2)	2543.1	0	46		300^{+360}_{-110}		$0.27^{+0.16}_{-0.15}$
		1902.1	641	31	$-0.19^{+0.13}_{-0.09}$		$4.6^{+2.8}_{-2.5}E-3$	$2.8^{+1.7}_{-1.5}E-2$
		1323.9	1219	23				$3.5^{+2.1}_{-1.9}$
5^+	2570.2(1)	1350.7	1219	87	$-0.56^{+0.12}_{-0.44}$	170^{+260}_{-80}	$4.6^{+3.5}_{-2.8}E-2$	$5.9^{+4.5}_{-3.6}$
		(827.4)	1743	13	$-0.44^{+0.18}_{-0.22}$		$3.5^{+2.6}_{-2.1}E-2$	$6.7^{+5.1}_{-4.0}$
3	2576.4(5)	1039.9	1537	24	$-0.69^{+0.29}_{-0.28}$	–		
		531.9	2045	31	$0.00^{+0.06}_{-0.09}$			
		297.8	2278	15	$0.85^{+0.19}_{-0.18}$			
		(394.0)	2182	19	$0.47^{+0.28}_{-0.31}$			
		(923.4)	1653	12				

TABLE I. (*Continued*).

J^π	E_x (keV)	E_γ (keV)	E_f (keV)	BR %	$\tan^{-1}(\delta)$ [a]	τ [b] (fs)	$B(M1)$ (W.u.)	$B(E2)$ (W.u.)
$^+$	2598.5(5)	2598.0	0	46		>2400		$<3.06E-2$
		1062.0	1537	54	$-0.25^{+0.10}_{-0.06}$		$<5.60E-3$	<0.19
$(3,2)^+$	2602.8(3)	1961.5	641	68	$0.03^{+0.03}_{-0.03}$	340^{+360}_{-120}	$8.3^{+4.6}_{-4.2}E-3$	$1.2^{+0.0}_{0.0}E-3$
		1383.3	1219	15	$0.85^{+0.19}_{-0.19}$		$2.3^{+1.3}_{-1.2}E-3$	$0.92^{+0.51}_{-0.47}$
		(1066.1)	1537	<4	$0.88^{+0.41}_{-0.41}$		$<1.4^{+0.8}_{-0.7}E-3$	$<1.0^{+0.6}_{-0.5}$
		557.7	2045	13			$6.8^{+0.1}_{-0.1}E-2$	
4^+	2606.6(1)	1965.2	641	14		70^{+120}_{-40}		$1.2^{+1.3}_{-0.8}$
		1387.1	1219	86	$0.85^{+0.13}_{-0.22}$		$6.1^{+6.6}_{-3.8}E-2$	$2.5^{+2.7}_{-1.5}E+1$
1	2667.4(4)	2667.0	0	49		78^{+35}_{-21}	$1.1^{+0.4}_{-0.3}E-2$	
		2026.1	641	30	"0"		$1.5^{+0.4}_{-0.3}E-2$	
		1130.9	1537	21	"0"		$5.9^{+0.4}_{-0.3}E-2$	
$(2-4)^+$	2680.6(2)	2039.2	641	100	$0.06^{+0.13}_{-0.09}$	210^{+210}_{-80}	$1.8^{+1.0}_{-0.9}E-2$	$9.0^{+10.}_{0.00}E-3$
$2,(3)^+$	2697.3(4)	2055.8	641	32	$-0.88^{+0.38}_{-0.38}$	120^{+80}_{-40}	$4.1^{+2.1}_{-1.7}E-3$	$0.84^{+0.44}_{-0.34}$
		1160.8	1537	27	$-0.19^{+0.16}_{-0.16}$		$4.5^{+2.4}_{-1.8}E-2$	$0.74^{+0.38}_{-0.30}$
		1044.1	1653	41			$BE1=1.1^{+0.6}_{-0.5}E-3$	
4^+	2698.6(2)	1479.2	1219	100	$0.91^{+0.06}_{-0.13}$	110^{+30}_{-22}	$3.3^{+0.8}_{-0.7}E-2$	$1.5^{+0.4}_{-0.3}E+1$
3^+	2715.4(4)	2073.7	641	30	$-0.03^{+0.06}_{-0.06}$	170^{+190}_{-70}	$6.2^{+3.9}_{-3.2}E-3$	$7.7^{+0.0}_{0.0}E-4$
		1495.8	1219	50	$0.35^{+0.06}_{-0.06}$		$2.4^{+1.5}_{-1.3}E-2$	$0.86^{+0.54}_{-0.44}$
		1178.8	1537	20	$-0.69^{+0.22}_{-0.19}$		$1.3^{+0.8}_{-0.7}E-2$	$3.9^{+2.5}_{-2.0}$
5^+	2725.8(1)	1506.4	1219	68	$0.09^{+0.04}_{-0.03}$	71^{+38}_{-23}	$8.8^{+4.1}_{-3.1}E-2$	$0.19^{+0.09}_{-0.07}$
		982.7	1743	32	$-0.13^{+0.19}_{-0.13}$		$0.15^{+0.07}_{-0.05}$	$1.6^{+0.7}_{-0.6}$
$2^{(-)}$	2728.1(4)	2086.6	641	42		390^{+420}_{-120}	$BE1=4.3^{+1.9}_{-2.2}E-5$	
		1191.6	1537	47			$BE1=2.6^{+1.1}_{-1.3}E-4$	
		1074.9	1653	11	$-1.10^{+0.19}_{-0.13}$		$1.5^{+0.6}_{-0.8}E-3$	$3.0^{+1.3}_{-1.6}$
(3,2)	2734.7(1)	2093.3	641	24	$1.38^{+0.09}_{-0.13}$	>530	$<5.7E-5$	$<2.1E-1$
		1515.4	1219	39	$-0.28^{-0.22}_{-0.15}$		$<6.3E-3$	<0.13
		1081.9	1653	14	$-0.09^{+0.12}_{-0.19}$		$<6.6E-3$	$<2.7E-2$
		(622.7)	2112	24	$0.19^{+0.22}_{-0.22}$			
(2,3)	2742.0(2)	2100.9	641	78	$-0.31^{+0.13}_{-0.13}$	110^{+40}_{-20}	$2.3^{+0.7}_{-0.6}E-2$	$0.32^{+0.09}_{-0.08}$
		1089.0	1653	22			$BE1=5.8^{+1.7}_{-1.5}E-4$	
(1–3)	2768.0(3)	2126.5	641	61	$-0.19^{+0.07}_{-0.07}$	80^{+26}_{-18}	$2.4^{+0.7}_{-0.6}E-2$	$0.12^{+0.03}_{-0.03}$
		1231.5	1537	22	$0.44^{+0.19}_{-0.16}$		$3.8^{+1.1}_{-0.9}E-2$	$3.3^{+0.9}_{-0.8}$
		1115.0	1653	17			$BE1=5.5^{+1.5}_{-1.3}E-4$	
(3)	2774.0(7)	1553.8	1219	17	$-0.75^{+0.34}_{-0.34}$	–		
		1237.6	1537	15	$0.38^{+0.18}_{-0.16}$			
		2133.3	641	52	$0.19^{+0.03}_{-0.06}$			
		(661.5)	2112	16	$0.19^{+0.22}_{-0.22}$			
(3–5)	2784.9(2)	1565.4	1219	100		330^{+910}_{-150}		
$1^{(+)}$	2801.0(5)	2800.4	0	11		14^{+3}_{-3}	$1.1^{+0.2}_{-0.2}E-2$	
		2160.0	641	56	"0"		$0.12^{+0.03}_{-0.02}$	
		1264.4	1537	33	"0"		$0.35^{+0.08}_{-0.06}$	
3^+	2806.6(5)	2164.8	641	42	$0.41^{+0.07}_{-0.03}$	140^{+100}_{-50}	$8.1^{+4.1}_{-3.4}E-3$	$0.19^{+0.10}_{-0.08}$
		1586.9	1219	17	$0.31^{+0.35}_{-0.25}$		$9.0^{+4.5}_{-3.8}E-3$	$0.22^{+0.11}_{-0.09}$
		1270.2	1537	41	$-0.16^{+0.07}_{-0.10}$		$4.5^{+2.3}_{-1.9}E-2$	$0.43^{+0.22}_{-0.18}$
(2,3)	2842.6(2)	2201.1	641	87	$-0.25^{+0.03}_{-0.13}$	55^{+14}_{-11}	$4.4^{+1.0}_{-0.9}E-2$	$0.35^{+0.08}_{-0.07}$
		1623.0	1219	12				$3.6^{+0.9}_{-0.7}$
		838.0	2005	<1				
2^+	2853.4(4)	2852.8	0	36		110^{+60}_{-30}		$0.34^{+0.14}_{-0.12}$
		2212.3	641	64	$-0.50^{+0.12}_{-0.19}$		$1.4^{+0.6}_{-0.5}E-2$	$0.50^{+0.21}_{-0.17}$
		1634.2	1219	<0.3				
4	2860.0(4)	1640.9	1219	22		–		
		1206.7	1653	78				

TABLE I. (*Continued*).

J^π	E_x (keV)	E_γ (keV)	E_f (keV)	BR %	$\tan^{-1}(\delta)$ [a]	τ [b] (fs)	$B(M1)$ (W.u.)	$B(E2)$ (W.u.)
(4)	2869.1(4)	(2228.3)	641	26		>657		<0.14
		1649.4	1219	35	$-0.41^{+0.28}_{-0.29}$		<3.2E−3	<0.13
		1216.1	1653	39			$BE1 < 1.2E-4$	
3	2887.8(1)	2246.4	641	78	$0.75^{+0.38}_{-0.16}$	59^{+17}_{-13}	$1.6^{+0.4}_{-0.4}E-2$	$2.5^{+0.7}_{-0.6}$
		1668.4	1219	22	$0.85^{+0.38}_{-0.34}$			
(2–4)	2934.0(9)	2292.7	641	100		>687		
		(1398.8)	1537					
3	2956.5(1)	2315.0	641	66	$-0.56^{+0.18}_{-0.41}$	24^{+10}_{-8}	$5.0^{+2.3}_{-1.5}E-2$	$2.2^{+1.0}_{-0.6}$
		1737.1	1219	34	$0.06^{+0.07}_{-0.09}$		$8.4^{+3.9}_{-2.5}E-2$	$6.0^{+3.0}_{-2.0}E-2$
1	2999.0(7)	2998.4	0	34		25^{+19}_{-12}	$BE1 = 1.8^{1.6}_{-0.8}E-4$	
		2358.3	641	66			$BE1 = 7.2^{6.5}_{-3.1}E-4$	
	3009.9(2)	2368.6	641	100		–		
1	3011.9(2)	3011.9	0	100		23^{+8}_{-6}		
(6)	3042.4(1)	1822.9	1219	54	$-0.35^{+0.09}_{-0.09}$	260^{+490}_{-110}	$9.8^{+7.4}_{-6.4}E-3$	$0.23^{+0.18}_{-0.15}$
		2401.0	641	46				
(3)	3052.0(2)	2410.3	641	12	$0.09^{+0.13}_{-0.12}$	–		
		1832.6	1219	23	$-0.79^{+0.22}_{-0.78}$			
		(1398.8)	1653	69				
		(864.6)	2188	0				
2,1(3)	3061.8(6)	2419.8	641	63	$-0.25^{+0.16}_{-0.15}$	130^{160}_{-60}	$9.9^{+6.9}_{-5.3}E-3$	$6.6^{+5.0}_{-4.0}E-2$
		1525.5	1537	37	$-0.09^{+0.15}_{-0.13}$		$2.5^{+1.7}_{-1.3}E-2$	$5.1^{+4.0}_{-3.0}E-2$
(2,3)	3089.9(2)	2448.4	641	72	$-0.69^{+0.19}_{-0.19}$	83^{42}_{-25}		
		(978.1)	2111	28				
3	3106.1(9)	2463.9	641	81	$-1.10^{+0.13}_{-0.06}$	76^{+38}_{-22}	$4.6^{+1.9}_{-1.5}E-3$	$1.8^{+0.7}_{-0.6}$
		1887.5	1219	19	$1.19^{+0.25}_{-0.94}$		$1.6^{+0.7}_{-0.5}E-3$	$1.7^{+0.7}_{-0.6}$
	3109.8(1)	2468.6	641	30		–		
		1890.3	1219	70				
(1–3)	3125.7(2)	2484.4	641	100		>943	<2.2E−3	
3	3144.9(4)	2503.1	641	49	$-0.69^{+0.19}_{-0.19}$			
		1608.4	1537	51	$-1.10^{+1.13}_{-0.13}$			
2^+	3153.6(1)	3153.6	0	35		160^{+220}_{-70}		$0.13^{+0.09}_{-0.07}$
		2512.4	641	65	$0.60^{+0.35}_{-0.34}$		$5.4^{+3.7}_{-3.1}E-3$	$0.24^{+0.16}_{-0.14}$
	3155.7(3)	1935.9	1219	50		–		
		1619.1	1537	50				
1	3180.5(3)	3180.2	0	100		–		
		2539.4	641					
3	3209.0(7)	2567.0	641	84	$-0.31^{+0.03}_{-0.07}$	62^{+59}_{-26}	$2.3^{+1.6}_{-1.1}E-2$	$0.21^{+0.15}_{-0.10}$
		1990.2	1219	16			$1.0^{+1.6}_{-1.1}E-2$	
	3218.2(2)	2576.9	641	100		–		
	3301.4(2)	1764.4	1537	100		–		

[a] In situations where χ^2 vs $\tan^{-1}(\delta)$ plots yield two equivalent solutions for the mixing ratio, the lower $\tan^{-1}(\delta)$ value has been used. The alternate solution leads to much larger $B(E2)$ rates and smaller $(M1)$ rates. The mixing ratio and $B(XL)$'s presented are those of the first spin listed when the spin of the initial state is not fixed. Angular distributions of $1^+ \rightarrow 2^+$ transitions are not sufficiently sensitive to the mixing ratio to allow a reliable determination. The mixing ratios for the 2398.7-keV state were taken from [12]. The mixing ratios for the 2667.4- and 2801.0-keV states are set to zero.

[b] Mean lifetimes for the 641.3- and 1219.5-keV states are taken from the literature. Lifetimes > 1 ps are too long to measure using the Doppler-shift attenuation method and are denoted by a "-."

864.6 keV originate from this level. The 864.6 keV assignment is tentative, and the 1398.6-keV line discussed above may also belong here.

We were unable to confirm transitions listed by Alhamidi *et al.* [13] for the following levels (transition energies): 2044.5 keV (390 keV), 2278.0 keV (272 keV), 2570.2 keV (827.4 keV), 2680.6 keV (1027 keV), 2697.3 keV (2697 keV), 2698.6 keV (586 keV), 2715.4 keV (671 keV), 2742.0 keV (2742 keV), 2887.8 keV (2888 keV), 2999.0 keV (1463 keV), 3061.8 keV (3061), 3089.9 keV (3091 keV), 3106.1 keV (1101 keV and 1569 keV), and 3153.6 keV (1618 keV). Transitions placed in the past of (467), 756, 864, 991, 1084, 1155, 1164, 1553, 1618, and 1689 keV belong to other levels according to our data. Additional new transitions were ob-

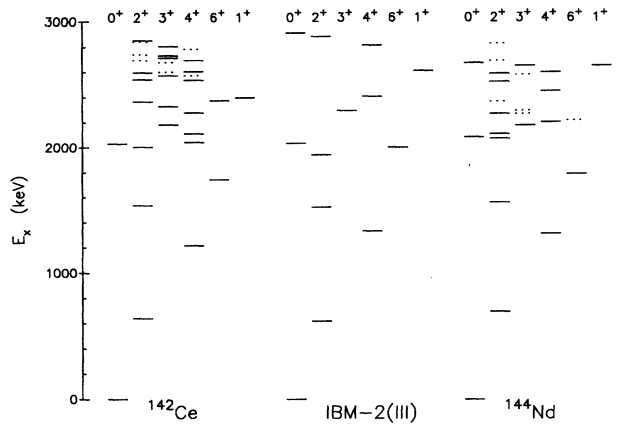

FIG. 4. Low-lying positive-parity levels of ^{142}Ce and ^{144}Nd. Results of the IBM-2(III) model calculations for ^{142}Ce are shown for comparison. The dotted lines represent levels with uncertain spins. Model calculations do not well reproduce the experimental level density above 2000 keV; this indicates that states above 2000 keV are expected to have a more complex structure than that represented by the the IBM-2.

served for the following levels (transition energies): 2728.1 keV (1074.9 keV), 2734.7 keV (622.7 keV), 2774.0 keV (1553.8 keV), 2742.0 keV (1089.0 keV), 2768.0 keV (1115.0 keV), and 2853.4 keV (1634.2 keV).

IV. DISCUSSION

A. General comments

The positive-parity levels of ^{142}Ce are shown in Fig. 4. The ratio $E_x(4_1^+)/E_x(2_1^+)=1.90$ and the quadrupole moment of the first excited state $Q(2_1^+)=-0.16(5)eb$ [10] are indicative of spherical vibrational character. The $E2$ transition rates for decays of the 0_2^+, 2_2^+, and 4_1^+ states into the 2_1^+ of 15 W.u., >19 W.u., and 27 W.u., respectively, although rather large and suggestive of some two-phonon character, are considerably less than the harmonic value, especially for the decay of the 0_2^+. The rather large energy separations among these three states suggests that anharmonicities are quite large. For example, the 0_2^+ state is pushed far up into the level scheme, above the 6_1^+ state that would be a member of the three-quadrupole phonon multiplet in a harmonic picture. Generally this behavior indicates gamma softness and a transition towards a gamma vibrator; the 2_2^+ lies above the 4_1^+ state which is not the expected 0-2-2 spin sequence of a gamma-unstable nucleus. More importantly, a true O(6) 0_2^+ state should decay only into the 2_2^+ state and not to the 2_1^+ state, which is exactly opposite to what is observed in this experiment; the decay from the 0_2^+ into the 2_2^+ has a branching ratio of $<1\%$.

Clearly existing experimental information indicates that the low-energy excitations cannot be explained by treating this nucleus purely as a simple spherical vibrator. To examine further the structure of ^{142}Ce, we compare below our experimental results with various model calculations. We are especially interested in the MS character of low-lying collective states, the possible fragmentation of MS strength, and multiphonon excitations. Extensive calculations for the $N=84$ isotones are available in the literature; we compare our experimental data with calculations made with the IBM-2, the particle-core coupling model (PCM), and the quasiparticle phonon model (QPM). We have made additional IBM-2 calculations for ^{142}Ce which are discussed thoroughly in the next section, and we use that model most extensively.

B. Model calculations

1. IBM-2 model calculations

The IBM-2 treats pairs of valence neutrons and pairs of valence protons as distinguishable bosons. This model is sufficiently well known that only details pertaining to ^{142}Ce calculations are given below.

Perhaps the most extensive set of existing IBM-2 calculations for the $N=84$ isotones was made by Copnell *et al.* [5]. Their IBM-2 calculations were performed using the code NPBOS [24] by iteratively fitting all known level energies, transition probabilities, and moments for each of the $N=84$ isotones from ^{138}Xe-^{146}Sm. Reasonable χ^2 fits were obtained by merely changing boson energies and boson numbers while fixing all other parameters in the NPBOS Hamiltonian [5] when going from one isotone to another. Effective charges and g factors were derived following the procedures in Refs. [25,26]. The number of proton and neutron bosons used in all ^{142}Ce calculations was $N_\pi=4$ and $N_\nu=1$, respectively. The following parameter set, which they [5] labeled IBM-2(I), was found for ^{142}Ce: $\epsilon=0.846$, $\kappa=-0.27$, $C_\pi^0=0.258$, $C_\pi^2=0.258$, $C_\pi^4=0.000$, $\xi_1=\xi_3=0.35$, and $\xi_2=0.1$, with $e_{\pi,\nu}=0.12$, $g_\pi=0.7$, $g_\nu=0.2$, $\chi_\pi=0.0$, and $\chi_\nu=-0.965$.

Using this same ^{142}Ce parameter set, for which we maintain the label IBM-2(I), and the same code NPBOS [24], we have extended the calculations to include additional states for which we now have experimental data. These new calculations reproduce rather well the level sequence and many transition rates; however, the IBM-2(I) parameter set is not successful with the energy spreading of the 0_2^+-2_2^+-4_1^+ triplet and with ground-state decays of many spin-2 states. These descrepancies motivated us to search for a refined parameter set which is more appropriate for ^{142}Ce.

The energy spacing of the two-phonon triplet was improved by varying the proton anharmonicity parameters C_π^L, $L=0,2,4$. The values obtained are $C_\pi^0=0.50$, $C_\pi^2=0.26$, and $C_\pi^4=-0.27$. The new C_π^4 value simultaneously improves the placement of the 4_1^+ and 6_1^+ states.

To increase the single-phonon character of the 2^+ states, terms in the Hamiltonian which do not conserve d-boson number were varied, e.g., the quadrupole-quadrupole interaction terms. There are two parameters associated with each term: κ and χ [5]. The parameter κ tends to control the single-phonon character of states, while χ influences the quadrupole moment. Modification of these coefficients did not improve the ground state $E2$ decay rates in a desirable fashion, since it appears that once the experimental $B(E2;2_1^+\rightarrow 0_1^+)$ value has been reproduced, there is not sufficient $E2$ strength left in the model to fit the other $B(E2)$

values. Variations of other parameters, while possible, did not seem merited.

We label the IBM-2(I) parameter set with the revised $C_\pi^{0,2,4}$ values as IBM-2(III). [The IBM-2(II) parameter set is discussed below.] This parameter set improves some level placements, as shown in Fig. 4, but transition rates remain relatively unaffected (typically $\leq 5\%$). Calculated transition rates are compared to the experimental values in Table II.

It is instructive to examine the overlap of the calculated IBM-2(III) wave functions with the harmonic U(5) wave functions. This comparison allows us to identify the spreading of MS strength in ^{142}Ce excited levels. These harmonic wave functions are generated by simply setting the quadrupole-quadrupole interaction κ and anharmonicity parameters C_π^L to zero and repeating the calculations. The resulting harmonic U(5) wave functions calculated are consistent with the analytic expressions given in Ref. [27]. Overlaps between the IBM-2(III) wave functions and the harmonic wave functions are given in Table III and discussed in more detail below.

Another parameter set labeled IBM-2(II) is available for ^{144}Nd from Copnell *et al.* [5]. The basic premise of the IBM-2(II) is that neutron and proton d bosons have different energies. This parameter set when used for ^{142}Ce predicts an even greater $B(E2;2_2^+ \rightarrow 0_1^+)$ value than does the IBM-2(I) parameters discussed above which leads to even more problems in describing other observed transitions. Because of these difficulties, we did not use this parameter set any further.

2. Existing PCM and QPM calculations

One might expect that nuclei near closed shells have experimental spectra strongly influenced by both collective and particle excitations. The QPM and the PCM take into account both these degrees of freedom but they do so in different ways. Extensive calculations for the $N=84$ isotones have been made using these models [5,6,20], especially for the low-lying 2^+ states.

The QPM is a microscopic random-phase approximation (RPA) model which uses a large basis of collective as well as two-quasiparticle (2QP) configurations [6]. The reader is referred to the work of Dinh *et al.* [6] and Kim *et al.* [20] for details. Dinh *et al.* [6] use the QPM to examine the interplay between collective and noncollective properties of low-lying quadrupole states and the fragmentation of collective strength in these states in four of the $N=84$ isotones. The QPM is also used by Kim *et al.* [20] to evaluate ^{142}Ce electron scattering data. Transition rates from Dinh *et al.* [6] are listed in Table II.

The PCM also takes into account both collective and particle degrees of freedom but quite differently than does the QPM. For ^{142}Ce the core excitations are the quadrupole and octupole collective vibrations in the ^{140}Ce nucleus, and the particles are the two valence neutrons which are coupled as single particles in the $N=82$–126 shell. Extensive calculations for the $N=84$ isotones from ^{138}Xe to ^{146}Sm have been made by Copnell *et al.* [5] using this model; parameters for each of the $N=84$ isotones are listed in Table III of Ref. [5]. Predictions from this model of $B(E2)$ and $B(M1)$ values for the three lowest 2^+ states and $B(E2)$ values for the 4_1^+ state in ^{142}Ce are listed in Table II.

We refer to existing ^{144}Nd PCM [5] and QPM [6] calculations for insight into the QP and phonon character of the wave functions for levels in ^{142}Ce. Calculations in both these references focused on ^{144}Nd because of the more extensive data set available for that nucleus. The level sequences of the two nuclei are so similar, as can be seen in the positive parity level comparison shown in Fig. 4, that we use the ^{144}Nd wave functions in our discussion of ^{142}Ce. Additionally, the authors of both Ref. [5] and Ref. [6] comment on the small differences in wave functions for neighboring isotones. Using wave functions calculated for ^{144}Nd to discuss ^{142}Ce is done with some caution, however, since QPM analyses of electron scattering data indicate that the underlying structure of the $N=82$ quadrupole vibrations is somewhat different for ^{140}Ce and ^{142}Nd [20].

C. States with mixed-symmetry character

Spin-2 states at 2–3 MeV excitation are predicted [9] to be the lowest states exhibiting MS character in vibrational nuclei. Decays of these quadrupole MS states are predicted to have small $E2/M1$ mixing ratios, as well as unusually large $M1$ transition rates to the lowest symmetric 2^+ state [4,9]. Strong $M1$ transitions from states of mixed symmetry to symmetric states have been the touchstone characteristic of isovector excitations in most theoretical models and were first observed in deformed nuclei for 1^+ states [4]. Observation of quadrupole MS states in ^{140}Ba, ^{142}Ce, and ^{144}Nd was first reported by Hamilton *et al.* [1]; the quadrupole MS strength had been attributed to a single state—the 2_3^+ level in each of these nuclei.

Fragmentation of isovector strength has been observed extensively in 1^+ MS states in deformed nuclei [4] and suggested for 2^+ states in the $N=84$ isotones [2,5,6,23]. Experimental information has not been extensive enough in the past to examine thoroughly the possible fragmentation of MS strength in vibrational nuclei or to look for higher lying 1^+ and 3^+ MS states. Our extended ^{142}Ce data set allows us to examine the MS character of such states. The systematics of $M1$ and $E2$ decay strengths for 2^+ and 3^+ states into the first excited state are shown in Fig. 5 and Fig. 6, respectively.

1. 1^+ states

The lowest IBM-2(III) 1^+ state contains 96% MS strength; however, the calculated $M1$ decay rate into the ground state is no larger than the average $B(M1)$ in this region. The measured $B(M1;1_1^+ \rightarrow 0_1^+)$ and $B(M1;1_1^+ \rightarrow 2_2^+)$ values are in good agreement with the IBM-2(III) calculations. The agreement is not as good for $B(M1;1_1^+ \rightarrow 2_1^+)$ and $E2$ decays.

The PCM predicts that the lowest 1^+ state contains substantial contributions from neutron two-particle states. The QPM calculations reported by Dinh *et al.* [6] do not investigate 1^+ states.

2. 2^+ states

Both the 2_3^+ 2004.9-keV state and the 2_4^+ 2364.9-keV state have rather large $M1$ transitions into the 2_1^+ level, which suggests that the low-lying MS strength is fragmented

TABLE II. Comparison of experimental and theoretical selected transition rates of ^{142}Ce. Uncertainties are those of the last digits and units are Weisskopf units. Each cell contains the experimental data followed by the calculated IBM-2(III) values. PCM and QPM predictions are available and included as the third and fourth entry, respectively, for the the lowest three 2^+ states and the 4_1^+ state.

	Final states					
Initial	0_1^+	2_1^+		2_2^+		4_1^+
State	$E2$	$M1$	$E2$	$M1$	$E2$	$E2$
0_2^+			15^{+8}_{-7}		–	
			12.8		2.48	
1_1^+	($M1=0.017^{+0.004}_{-0.004}$)	$0.0022^{+0.0006}_{-0.0005}$	$1.0^{+0.3}_{-0.2}$	$0.036^{+0.010}_{-0.009}$	$0.026^{+0.007}_{-0.006}$	
	($M1=0.0160$)	0.0076	< 0.02	0.0332	2.36	
2_1^+	$21.2^{+2.4}_{-1.9}$					
	23.4					
	17					
	16.8					
2_2^+	>0.023	>0.012	>19			–
	0.486	0.0116	22.1			1.16
	0.0231	0.0246	8.10			
	0.0045	0.022	27.3			
2_3^+	$2.5^{+0.2}_{-0.2}$	$0.13^{+0.01}_{-0.01}$	$2.6^{+0.3}_{-0.3}$	–	–	–
	< 0.02	0.0302	3.43	0.0066	2.13	2.78
	2.08	0.0140	1.62			
	2.27	0.20	6.82			
2_4^+	$2.6^{+0.4}_{-0.3}$	$0.20^{+0.03}_{-0.03}$	$0.037^{+0.006}_{-0.005}$	–	–	–
	< 0.02	0.0000	< 0.02	0.0045	3.15	2.43
2_5^+	$0.27^{+0.16}_{-0.15}$	$0.0046^{+0.0028}_{-0.0025}$	$0.028^{+0.017}_{-0.015}$	–	–	$3.5^{+2.1}_{-1.9}$
	< 0.02	0.0025	< 0.02	0.0016	<0.02	1.16
3_1^+		$0.0088^{+0.0066}_{-0.0060}$	$0.018^{+0.013}_{-0.012}$	$0.032^{+0.024}_{-0.022}$	$7.3^{+5.4}_{-4.9}$	$5.0^{+3.7}_{-3.4}$
		0.0031	0.72	0.0078	26.8	8.77
3_2^+		$0.015^{+0.009}_{-0.008}$	$0.082^{+0.047}_{-0.042}$	$0.056^{+0.032}_{-0.029}$	$7.1^{+4.1}_{-3.6}$	–
		0.0018	<0.0231	0.0085	0.30	1.53
4_1^+			$27.^{+3}_{-2}$			
			32.3			
			14.1			
			22.7			
4_2^+			$7.2^{+2.0}_{-1.8}$		Obscured	$0.011^{+0.003}_{-0.003}$
			0.16		14.9	12.3
4_3^+			–		Very weak	$10.0^{+4.7}_{-4.5}$
			0.67		< 0.02	1.04
4_4^+			$9.7^{+3.21}_{-2.74}$		–	$22.00^{+9.48}_{-8.11}$
			0.05		<0.02	0.30

TABLE III. Overlaps of IBM-2(III) and harmonic U(5) wave functions for states below 3700-keV excitation.

Harmonic	*n*th IBM-2(III) state				
U(5) states	1	2	3	4	5
			Spin 0		
0_1^+	0.860	-0.401	0.102	0.284	
$0_2^+(d^2)$	-0.411	0.798	-0.252	0.225	
$0_3^+(d^2)$	0.284	-0.084	-0.446	-0.680	
$0_4^+(d^3)$	0.083	0.299	-0.824	0.418	
			Spin 2		
$2_1^+(d)$	-0.888	0.207	-0.140	0.281	0.129
$2_2^+(d^2)$	0.215	0.804	-0.432	-0.067	-0.144
$2_3^+(d^3)$	-0.300	0.144	0.340	-0.637	-0.485
$2_m^+(d)$	0.131	0.462	0.744	-0.113	0.321
$2_m^+(d^2)$	-0.108	-0.115	-0.165	-0.610	0.597
$2_{m1}^+(d^3)$	0.213	-0.101	-0.150	-0.025	-0.165
$2_{m2}^+(d^3)$	-0.138	0.138	0.097	0.018	0.005
$2_{m3}^+(d^3)$	-0.042	-0.056	0.070	-0.155	0.120
			Spin 3		
$3_1^+(d^2)$	-0.627	0.700	-0.231		
$3_2^+(d^3)$	-0.744	-0.612	-0.030		
$3_3^+(d^3)$	-0.087	0.287	0.116		
$3_4^+(d^3)$	-0.176	0.094	0.939		
			Spin 4		
$4_1^+(d^2)$	-0.916	0.126	-0.253	0.149	
$4_2^+(d^2)$	-0.062	-0.411	0.738	-0.014	
$4_3^+(d^3)$	0.198	-0.863	-0.337	-0.037	
$4_4^+(d^3)$	-0.060	-0.064	-0.231	-0.125	

over these two levels which are split by about 300 keV. The summed $M1$ strength of these decays into the first excited state of $B(M1)=0.59(6)\mu_N^2$ is larger than the maximum value in the vibrational limit of the IBM-2 of $B(M1;2_{MS}^+\rightarrow 2_1^+)\simeq 0.23\mu_N^2$ [27]. The summed $E2$ decay strength into the ground state is also significantly larger than the predicted value of $B(E2;2_{MS}^+\rightarrow 0_1^+)=0.6$ W.u [9].

Examination of the calculated IBM-2(III) wave functions shows clearly that the one d boson $2_M(d)$ is fragmented over the second, third, and fifth 2^+ states, with the 2_3^+ receiving the largest contribution of $\approx 55\%$. The two d-boson $2_M(d^2)$ strength is split between the fourth and fifth 2^+ states. The model underpredicts the ground-state decay rates of the 2_3^+ and 2_4^+ states. This feature cannot be corrected by altering the model parameters, which suggests that these states require particle degrees of freedom in addition to the vibrational configurations.

Dinh *et al.* [6] examine the three lowest quadrupole states using the QPM. They find the lowest 2^+ state is predominantly a single-phonon collective state, while the 2_2^+ state has a large two-phonon component. They also find that isovector strength is shared between the 2_2^+ and 2_3^+ states, in very good agreement with our results for transition rates.

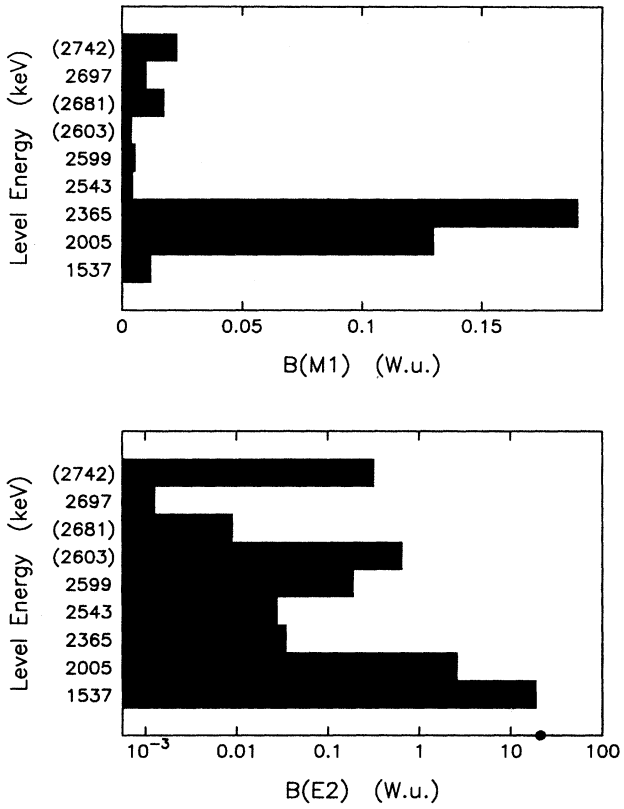

FIG. 5. Systematics of $M1$ and $E2$ decays of 2^+ levels into the 2_1^+ state in ^{142}Ce. Large $M1$ transitions are clearly observed from the 2_2^+ and 2_3^+ states. For comparison, the $B(E2)$ rate of the first excited state is indicated by the dot on the horizontal axis.

Unfortunately, the QPM calculations did not include any higher-lying 2^+ states.

The PCM calculations for ^{142}Ce by Copnell *et al.* [5] are in quite good agreement with the measured ground-state decay rates of the first three 2^+ states as well as the other decays of the 2_3^+ state. Decay of the symmetric two-phonon 2_2^+ state into the first excited state is, however, significantly underestimated. PCM wave functions are presented in Ref. [5] for the neighboring nucleus ^{144}Nd. There the lowest three 2^+ states were composed of recoupled $f_{7/2}$ neutrons and a single $N=82$ phonon coupled to the lowest two-neutron configurations. The 2_2^+ state was not predicted to have significant two-phonon character.

Calculated and experimental transition rates for the five lowest 2^+ states can be seen in Table II. Theoretical values from the QPM and PCM are given only for the three lowest 2^+ states. None of the models does well describing both ground-state decays and decays to the 2_1^+ level.

3. 3^+ states

For spin-3 states, the measured $M1$ strengths are all comparable and small and no clear identification of MS candidates can be made on the basis of experimental information. The IBM-2(III) calculations indicate that the lowest $3_m^+(d^2)$ strength is split between the first and second 3^+ states. Mani-

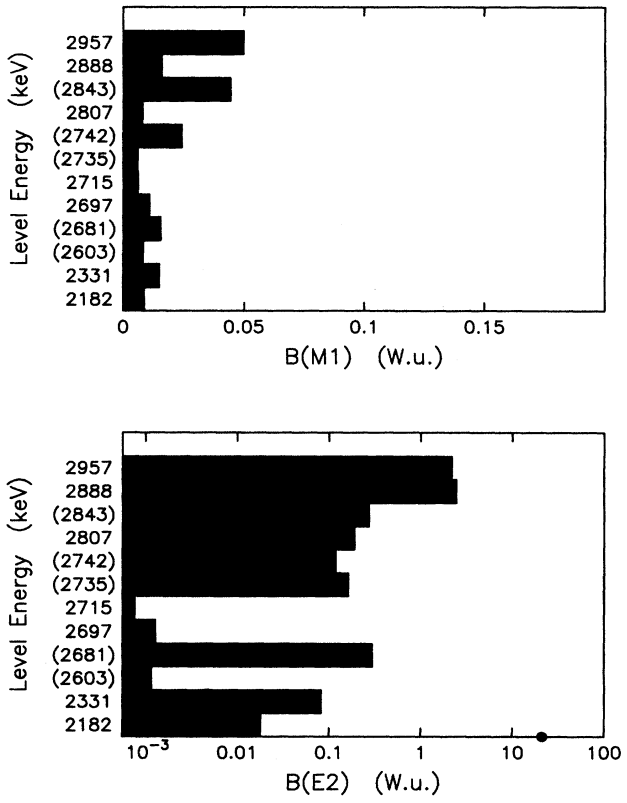

FIG. 6. Systematics of $M1$ and $E2$ decays of 3^+ levels into the 2_1^+ state in ^{142}Ce. None of the low-lying 3^+ states are characterized by large $M1$ transitions into the 2_1^+ level. For comparison, the $B(E2)$ rate of the first excited state is indicated by the dot on the horizontal axis.

festations of this split are small $M1$ transitions and sizeable $E2$ transitions into the 2_2^+ and 4_1^+ states. For the most part this is what is observed, although the magnitudes of the measured $E2$ transition rates are not in good agreement with the IBM-2(III) predictions. This is a situation where the presence of isovector strength does not manifest itself directly in terms of strong $M1$ decays into symmetric states; it is only implied in the calculations.

D. Multiphonon structures

1. Two-quadrupole phonon structures

The triplet of states $(0^+,2^+,4^+)$ predicted from the coupling of two quadrupole phonons is expected to occur at twice $E(2_1^+)$ in a simple vibrational picture. Candidates for members of this multiplet are described below.

0_2^+ 2031.0 keV. The experimental $B(E2;0_2^+\rightarrow 2_1^+)$ is reproduced well by IBM-2 calculations, which predict that the wave function for this state is composed of ≈64% two-phonon components. The overlap between the IBM-2 and PCM wave functions for this state is only about 35% which indicates that the two models predict very different structure for this level [5]. The success of the IBM-2 calculations in reproducing our measured $E2$ transition rate suggests that this state is more collective than PCM calculations predict.

2_2^+ 1536.9 keV. The IBM-2 calculations for this state do quite well with the $E2$ transition rate for the decay into the first excited state but vastly overpredict the ground-state $E2$ rate. The IBM-2 wave function for this level indicates that it is comprised of 66% two-phonon and 26% single-phonon configurations. The experimental transition rate seems to suggest that the model predicts too much single-phonon character.

The PCM has the opposite problem since it correctly predicts the ground-state branch, but the $E2$ rate to the 2_1^+ is underestimated by more than a factor of 2. The lack of two-phonon components in the PCM wave function for the 2_1^+ offers the most obvious explanation, especially since strong two-phonon character of this state is supported by electron scattering data and QPM calculations [7].

QPM calculations underpredict the ground-state decay and overpredict both the $M1$ and $E2$ decay strength into the 2_1^+. This suggests that the one-phonon component of this state is too small while the two-phonon strength is too large in this model.

4_1^+ 1219.5 keV. The 4_1^+ excitation energy and its $E2$ transition rate into the first excited state suggest that this state has strong two-phonon character. The IBM-2 calculations do rather well reproducing this experimental rate. The PCM underpredicts the 4_1^+ $E2$ decay rate by about a factor of 2, which again can be explained by a lack of two-phonon components in the PCM wave functions.

The QPM slightly underpredicts the $B(E2;4_1^+\rightarrow 2_1^+)$ value. Calculations by Dinh *et al.* [6] for the 4_1^+ state indicate it is composed of approximately 65% one-phonon and approximately 30% two-phonon components.

The 4_1^+ state has previously been examined in the $N=84$ isotone ^{144}Nd by Cottle *et al.* [23]. Systematics of 4_1^+ states in this mass region indicate that they are primarily of 2QP nature near $N=82$ and rotational in the $N=90$ nuclei. The 2QP nature of the 4_1^+ state in the core $N=82$ nuclei comes from couplings of protons in the $d_{5/2}$ and $g_{7/2}$ orbits [23].

Electron scattering measurements [20] found $B(E4;4_1^+\rightarrow 0_1^+)=14.3$ W.u. for ^{142}Ce, which is similar to the value of $B(E4;4_1^+\rightarrow 0_1^+)=12$ W.u. found for ^{144}Nd [23]. Analyses of proton scattering data by Cottle *et al.* [23] for ^{144}Nd showed rather conclusively both one-step particle excitations and two-step processes were needed to describe the scattering to this state. Their analysis also indicated that single-phonon excitations did not play a large role in the excitation of this state in ^{144}Nd. For ^{144}Nd the ratio [23] $B(E2;4_1^+\rightarrow 2_1^+)/B(E2;2_1^+\rightarrow 0_1^+)$ is 0.2, which is considerably less than the same ratio in ^{142}Ce.

From the differences in the transition rates for these two nuclei it appears that the 4_1^+ state in ^{142}Ce has more two-phonon strength than does the same state in ^{144}Nd, although both nuclei have similar $B(E4;4_1^+\rightarrow 0_1^+)$ values. The enhanced collective nature of ^{142}Ce may result from the number of active protons participating in the interaction. Calculations for the $N=84$ isotones by Copnell *et al.* [5] indicate that there are more active protons in ^{142}Ce than in ^{144}Nd because of the presumed shell closure at $Z=64$.

2. Three-quadrupole phonon structures

From large anharmonicities observed in the two-phonon excitations, three quadrupole-phonon (3Q) strength in ^{142}Ce is expected to be fragmented over several levels. This fragmentation makes identification of members of the quintet difficult. The signature of such states should be strong $E2$ decays into two-phonon states. The centroid of the 3Q strength should be near three times $E_x(2_1^+)$, or $\simeq$1.9 MeV. We have identified possible candidates for most members of the the 3Q quintet.

3Q 0^+ state. No high-lying spin-0 states have been identified in this nucleus.

3Q 2^+ state. Spin-2 states with rather strong decays into the 4_1^+ lie at 2543.3 and 2602.8 keV. The 2602.8 keV state may also decay rather strongly into the 2_2^+ state. The $B(E2)$ rate of the decay of the lower state is about twice the combined rates for the decay of the 2_2^+ state.

3Q 3^+ state. The first and second 3^+ states at 2182.1 keV and 2330.5 keV have rather strong $E2$ decays into the second 2^+ state. In addition, the 2182.1 keV state has a strong $E2$ decay into the lowest 4^+ state. This suggests the presence of a significant three-phonon component in the wave functions of these states.

3Q 4^+ state. Both the 4_3^+ at 2112.0 keV and 4_4^+ at 2278.0 keV have strong $E2$ transitions into the first 4^+ state; however, neither has a measureable decay into the 2_2^+. A state with a strong B(E2;$4^+ \rightarrow 2_2^+$) is the 4_5^+ at 2540.2 keV, but no decay was observed to the lowest spin-4 state.

3Q 6^+ state. Spin-6 states occur at 1743.0 and 2374.9 keV. Of these, the low-lying 1743.0 keV state is the most likely 3Q candidate because of energetics.

3. Quadrupole-octupole coupled structures

Coupling between single quadrupole and octupole vibrational modes will produce a quintet of levels with spins 1^- – 5^-. In a simple vibrational model these states should lie at an energy given by the sum of $E(2_1^+)$ and $E(3_1^-)$, which is $\simeq$2200 keV in ^{142}Ce. Candidates for these states have been identified in a few other nuclei in this mass region; the best examples are in ^{144}Sm [28] and ^{144}Nd [29]. Ideally $E3$ transitions from this quintet of states into the 2_1^+ and $E2$ transitions into the 3_1^- should have $B(E3)$ and $B(E2)$ values of the same strength as $B(E3;3_1^- \rightarrow 0_1^+)$ and $B(E2;2_1^+ \rightarrow 0_1^+)$, respectively [29]. In practice one usually cannot see large $E3$ strengths into the single phonon states, because decays are dominated by rather strong $E1$ transitions. Identification of the quadrupole-octupole coupled (QOC) candidates in ^{142}Ce is guided by decay patterns and model calculations in neighboring nuclei [29–31].

QOC 1^- state. Spin-1 states of interest lie at 2187.6- and 2542.8- keV excitation. The state at 2542.8 keV is known to have a short lifetime, probably less than 20 fs, but the parity has not been determined. Electron scattering [7] has suggested a 1^- state at 2742 keV, but this state has been assigned spin 2 or 3 by $(n,n'\gamma)$ studies [13].

Robinson *et al.* [29] report that the 1_1^- state at 2186.7 keV in ^{144}Nd has decay characteristics supporting the QOC structure of this state. Our measured $E1$ rates of the 2187.6 keV state into the 0_1^+ and 2_1^+ are of the same strength as those measured for the 1_1^- state in ^{144}Nd. Hartree-Fock calculations by Vogel and Kocbach [30] are consistent with this assignment; therefore, we similarly choose the 2187.6-keV state in ^{142}Ce as the QOC candidate.

QOC 2^- state. States with spin and parity of 2^- are rare and difficult to identify in nuclei. In γ-decay studies, negative parity would be indicated by a $L=1,2$ transition into the 3_1^- with a nonzero mixing ratio. Spin-2 states of interest are 2728.1, 2734.7, 2742.0, and 2768.0 keV. The last two states are observed in (e,e') [7] and are therefore of natural parity. The state at 2734.7 keV excitation is observed to decay into the 4_1^+ level. This would be an $M2$ decay if the 2734.7 is the 2_1^-, and such decays are not common. The state at 2728.1 keV is the most likely candidate for the QOC 2^- candidate. This is supported experimentally since there are two solutions for the 2728.1 keV $\rightarrow$ 3_1^- mixing ratio: $\tan^{-1}\delta = -0.31^{+15}_{-19}$ or -1.10^{+19}_{-13} either possibility yields a sizeable $E2$ component which indicates the state is definitely 2_1^-.

QOC 3^- state. There are several spin-3 states between 2.6 and 3.0 MeV in this nucleus. Based on the location of other QOC candidates and decay patterns, possible candidates are the levels at 2697.3, 2734.7, 2742.0, 2768.0, and 2774.0 keV. Choosing among these is difficult. The preferred spin assignment for the 2697.3 keV state is 2^+ [7]. The angular distributions of the decays from 2734.7 and 2774.0 keV levels into positive parity states do not consistently show the negative a_2 Legendre coefficients generally expected for $E1$ transitions. The states at 2742.0 and 2768.0 are known to have natural parity based on their observation in electron scattering and are the most likely candidates. The 2768.0 keV level does decay into the 3_1^- with $B(E2) < 3.62$ W.u. (A background line at 1231 keV prohibits a definite evaluation of this transition rate.)

QOC 4^- state. The spin-4 level at 2384.5 keV was assigned negative parity based on characteristic γ decays, systematics of the $N=84$ nuclei [19], and reanalysis of earlier reactor $(n,n'\gamma)$ data by Alhamidi *et al.* [13]. Decay into the 3_1^- is readily observed and the mixing ratio of the transition indicates a large $E2$ component. Any possible $E3/M2$ decay into the first excited state would be too weak to be observed. No lower-lying 4^- state was observed making this the most likely member of the QOC quintet.

QOC 5^- state. The only observed 5^- level below 3.1 MeV lies at 2124.9 keV. A very strong $E2$ transition from this state into the 3_1^- state is observed. This state also has $E1$ decays into the 4_1^+ and 6_1^+ states. The lifetime of this state can be derived from the 905.6 keV transition, but this γ-ray energy is at the lower limit of our ability to observe Doppler shifts and uncertainties are rather large. This state is the most likely candidate for the 5^- member of the QOC quintet.

Direct excitation investigations of the 5^- candidate in ^{144}Nd by Cottle *et al.* [32] indicate that single-step processes are strong and, therefore, these states have large 2QP structure. Robinson *et al.* [29] propose that this state in ^{144}Nd has about equal contributions of QOC and 2QP character in its structure.

V. SUMMARY

The excited levels of ^{142}Ce and the electromagnetic transitions between these levels have been studied using the $(n,n'\gamma)$ reaction. Excitation functions, angular distributions, and Doppler shifts were measured for γ rays for levels up to an excitation energy of 3.3 MeV; multipole mixing and branching ratios and lifetimes were deduced for many decays.

The spreading of MS strength in 2^+ states was discovered by examining experimental $B(M1)$ and $B(E2)$ values for decays from MS to symmetric states. Both the 2004.9-keV and 2364.9-keV 2^+ states have rather large $M1$ transitions into the 2_1^+ state, which suggests that the low-lying quadrupole MS strength is largely fragmented over just these two levels. IBM-2 calculations support the fragmentation of MS strength in these two levels as well as in the 2_5^+ state. This model does an excellent job reproducing the measured transition rates from the 2_1^+ and 2_2^+ states, but badly underpredicts the ground-state decays of the 2_3^+ and 2_4^+. Some features, such as these ground-state decays of higher lying 2^+ states, lie outside the limits of the IBM-2 model and appear to require a more particlelike interpretation. For spin-3 states no clear identification of MS candidates can be made from the experimental information, but IBM-2 calculations show clearly that the MS strength is expected to be split between the first and second 3^+ states.

Existing PCM and QPM model calculations were compared to our experimental data for transitions from low-lying 2^+ states. The PCM was more successful than the IBM-2 in predicting ground state $E2$ rates, but decays into the 2_1^+ state are significantly underestimated. This seems to indicate that the PCM does not contain enough collective strength to describe these transitions. Quasiparticle phonon calculations for the lowest 2^+ states show clearly a fragmentation of MS strength between the 2_2^+ and 2_3^+ states in good agreement with our data. The QPM calculations do rather well reproducing $B(E2;2_3^+\rightarrow 0_1^+)$ and $B(E2;4_1^+\rightarrow 2_1^+)$, but the agreement with other experimental transition rates is not as good.

Clearly, none of the models do an excellent job reproducing all the observed transition rates. Equally clear is the need to include both particle and collective degrees of freedom in describing the ^{142}Ce excitations.

Finally, we have identified candidates for the two quadrupole-phonon triplet, the three quadrupole-phonon quintet, and the quadrupole-octupole phonon coupled quintet.

ACKNOWLEDGMENTS

The support of the National Science Foundation for this project through Grants No. PHY-9303345 and No. PHY-9302914 is gratefully acknowledged. We also acknowledge with appreciation discussions with M. T. McEllistrem and S. W. Yates of the University of Kentucky.

[1] W. D. Hamilton, A. Irbäck, and J. P. Elliott, Phys. Rev. Lett. **53**, 2469 (1984).
[2] R. A. Meyer, O. Scholten, S. Brant, and V. Paar, Phys. Rev. C **41**, 2386 (1990).
[3] R. Nojarov and A. Faessler, J. Phys. G **13**, 337 (1987).
[4] P. O. Lipas, P. von Brentano, and A. Gelberg, Rep. Prog. Phys. **53**, 1355 (1990).
[5] J. Copnell, S. J. Robinson, J. Jolie, and K. Heyde, Phys. Rev. C **46**, 1301 (1992).
[6] Thai Khac Dinh, M. Grinberg, and C. Stoyanov, J. Phys. G **18**, 329 (1992).
[7] W. Kim, J. R. Calarco, J. P. Connelly, J. H. Heisenberg, F. W. Hersman, T. E. Milliman, J. E. Wise, B. L. Miller, C. N. Papanicolas, V. Yu. Ponomarev, E. E. Saperstein, and A. P. Platonov, Phys. Rev. C **44**, 2400 (1991).
[8] W. J. Vermeer, C. S. Lim, and R. H. Spear, Phys. Rev. C **38**, 2982 (1988).
[9] F. Iachello, Phys. Rev. Lett. **53**, 1427 (1984).
[10] R. H. Spear, W. J. Vermeer, S. M. Burnett, G. J. Gyapong, and C. S. Lim, Aust. J. Phys. **42**, 345 (1989).
[11] E. Michelakakis, W. D. Hamilton, P. Hungerford, G. Jung, B. Pfeiffer, and S. M. Scott, J. Phys. G **8**, 111 (1982).
[12] A. L. Lapolli, C. B. Zamboni, and R. N. Saxena, Phys. Rev. C **41**, 2312 (1990).
[13] M. M. Alhamidi, A. M. Demidov, M. M. Dufani, M. S. Elahrash, V. A. Kurkin, I. V. Mikaĭlov, J. M. Rateb, S. M. Sergiwa, A. M. Shermit, and S. M. Zleetni, Sov. J. Nucl. Phys. **55**, 496 (1992).
[14] B. Fazekas, T. Belgya, G. Molnár, Á. Veres, R. A. Gatenby, S. W. Yates, and T. Otsuka, Nucl. Phys. **A548**, 249 (1992), and references therein.
[15] E. Sheldon and D. M. van Patter, Rev. Mod. Phys. **38**, 143 (1966).
[16] H. S. Camarda, T. W. Phillips, and R. M. White, Phys. Rev. C **29**, 2106 (1984).
[17] K. B. Winterbon, Nucl. Phys. **A246**, 293 (1975).
[18] T. Belgya, B. Fazekas, G. Molnár, R. A. Gatenby, E. L. Johnson, E. M. Baum, D. Wang, D. P. DiPrete, and S. W. Yates, in *Proceedings of the 8th International Symposium on Capture Gamma-Ray Spectroscopy and Related Topics*, Fribourg, Switzerland, 1993, edited by J. Kern (World Scientific, Singapore, 1994), p. 878.
[19] L. K. Peker, Nucl. Data Sheets **43**, 579 (1984).
[20] W. Kim, B. L. Miller, J. R. Calarco, L. S. Cardman, J. P. Connelly, S. A. Fayans, B. Frois, D. Goutte, J. H. Heisenberg, F. W. Hersman, V. Meot, T. E. Milliman, P. Mueller, C. N. Papanicolas, A. P. Platonov, V. Yu. Ponomarev, and J. E. Wise, Phys. Rev. C **45**, 2290 (1992).
[21] T. J. Mulligan, E. R. Flynn, O. Hansen, R. F. Casten, and R. K. Sheline, Phys. Rev. C **6**, 1802 (1972).
[22] G. Engler, Phys. Rev. C **1**, 734 (1970).
[23] P. D. Cottle, S. M. Aziz, K. W. Kemper, M. L. Owens, E. L. Reber, J. D. Brown, E. R. Jacobsen, and Y. Y. Sharon, Phys. Rev. C **43**, 59 (1991).
[24] T. Otsuka and N. Yoshida, Japanese Atomic Energy Research Institute Report No. 85-094 (1985).

[25] S. J. Robinson, J. Copnell, J. Jolie, U. Stöhlker, and V. Rabbel, in *Proceedings of the 6th International Symposium on Capture Gamma-Ray Spectroscopy,* Leuven, Belgium, 1987, edited by K. Abrahams and P. Van Assche, IOP Conf. Series No. 88 (IOP, London, 1987), p. 506.

[26] M. Sambataro, O. Scholten, A. E. L. Dieperink, and G. Piccitto, Nucl. Phys. **A423**, 333 (1984).

[27] P. Van Isacker, K. Heyde, J. Jolie, and A. Sevrin, Ann. Phys. (N.Y.) **171**, 253 (1986).

[28] R. A. Gatenby, J. R. Vanhoy, E. M. Baum, E. L. Johnson, S. W. Yates, T. Belgya, B. Fazekas, Á. Veres, and G. Molnár, Phys. Rev. C **41**, R414 (1990).

[29] S. J. Robinson, J. Jolie, H. G. Börner, P. Schillebeeckx, S. Ulbig, and K. P. Lieb, Phys. Rev. Lett. **73**, 412 (1994).

[30] P. Vogel and L. Kocbach, Nucl. Phys. **A176**, 33 (1971).

[31] M. Pignanelli, N. Blasi, J.A. Bordewijk, R. De Leo, M. N. Harakeh, M. A. Hofstee, S. Micheletti, R. Perrino, V. Yu. Ponomarev, V. G. Soloviev, A. V. Sushkov, and S. Y. van der Werf, Nucl. Phys. **A559**, 1 (1993).

[32] P. D. Cottle, K. W. Kemper, M. A. Kennedy, L. F. Fifield, and T. R. Ophel, Phys. Rev. C **47**, 1048 (1993).